Journal of the Physical Society of Japan **85**, 091006 (2016)
http://doi.org/10.7566/JPSJ.85.091006

μSR Studies on Magnetism in High-T_c Cuprates

Yoji Koike[1*] and Tadashi Adachi[2]

[1]*Department of Applied Physics, Graduate School of Engineering, Tohoku University, Sendai 980-8579, Japan*
[2]*Department of Engineering and Applied Sciences, Sophia University, Chiyoda, Tokyo 102-8554, Japan*

(Received November 13, 2015; accepted November 20, 2015; published online July 1, 2016)

Since the discovery of high-T_c superconductivity in cuprates, muon spin relaxation (μSR) measurements have greatly contributed to the understanding of high-T_c superconductivity. In this paper, μSR studies on the magnetism in high-T_c cuprates obtained these past three decades are reviewed. Antiferromagnetic long-range order, 1/8 anomaly, stripes of Cu spins and holes, impurity-induced magnetism, magnetic-field-induced magnetism, pseudogap, ferromagnetism in the heavily overdoped regime, and undoped superconductivity in T′-type cuprates are discussed. Moreover, the fundamentals of μSR measurements for the study of magnetism are described for μSR beginners.

1. Introduction

Three decades have passed since the discovery of high-T_c superconductivity in cuprates.[1)] Muon spin relaxation (μSR) is a powerful experimental technique for studying the magnetism in strongly correlated electron systems, playing a complementary role as well as neutron scattering and nuclear magnetic resonance (NMR). In fact, μSR measurements have greatly contributed to the understanding of the high-T_c superconductivity in cuprates regarded as strongly correlated electron systems. In this paper, to begin with, the fundamentals of μSR measurements for the study of magnetism are described for μSR beginners. Then, μSR studies on the magnetism in high-T_c cuprates obtained these past three decades are reviewed as follows. First, μSR studies on the determination of the phase diagram, namely, the carrier-concentration dependence of the Néel temperature T_N of the antiferromagnetic (AF) long-range ordered phase adjacent to the superconducting phase are shown. Second, μSR studies on the so-called 1/8 anomaly, namely, the anomalous suppression of superconductivity at the hole concentration of 1/8 per Cu and related stripes of Cu spins and holes in hole-doped high-T_c cuprates are described. Third, μSR studies on the impurity-induced magnetism and its relation to the suppression of the superconductivity in hole-doped cuprates are shown. Fourth, μSR studies on the magnetic-field-induced magnetism are described. Fifth, μSR studies on the pseudogap phase in hole-doped cuprates are shown. Sixth, μSR studies on the ferromagnetism in the heavily overdoped non-superconducting regime of hole-doped cuprates are described. Finally, very recent μSR studies on the undoped superconductivity in cuprates with the so-called T′-type structure without excess apical oxygen are described.

2. Fundamentals of μSR Measurements for μSR Beginners

A muon is an elementary particle with the spin quantum number $s = 1/2$, and therefore, with the magnetic moment $m = \gamma_\mu \hbar s$, where $\gamma_\mu = 2\pi \times 13.55$ kHz/G and $\hbar$ is the Planck constant divided by 2π. Accordingly, muons are useful for obtaining information on the internal magnetic field of a material. Here, only the fundamentals of μSR measurements for the study of magnetism, namely, the minimum knowledge necessary to understand μSR time spectra using positively charged muons μ^+ are described for μSR beginners.

(1) Positive muons 100% spin-polarized along the injection direction are injected into a material.

(2) A positive muon stops at the site, where the electrostatic potential is the lowest, near a negative ion in a material. Note that muons are not fixed at the site but diffuse in a material at high temperatures, for example, above ~200 K in cuprates.

(3) Feeling the internal magnetic field H at the stopping site in a material, a muon makes a Larmor precession with the angular frequency $\omega = \gamma_\mu H$.

(4) The lifetime of positive muons is 2.2 μs: the half-life is 1.5 μs. A positive muon μ^+ decays to be a positron e^+ traveling in the direction of the μ^+ spin at the moment of the decay in the highest probability.

(5) The difference between counted numbers of forward and backward counters of e^+ located around a material is called asymmetry and indicates the polarization rate of μ^+ spins. From the asymmetry at each time, one can know the direction of spins of μ^+ decaying at each time.

(6) The lives of muons stopping in a material are different muon by muon. The μSR time spectrum is composed of data of the asymmetry $A(t)$, namely, the polarization rate of μ^+ spins at the time t from the stop of μ^+ in a material to the decay of μ^+, namely, to the detection of e^+ by the counter, as shown in Fig. 1.

(7) The μSR time spectrum indicates the statistical average of the time development of the direction of μ^+ spins, namely, the Larmor precession. Therefore, the S/N of the μSR time spectrum increases with increasing number of muons stopping in a material. Since the number of muons with short lives is statistically larger than that with long lives, the S/N in a short-time region is better than that in a long-time region.

(8) In the case of no internal magnetic field, μ^+ spins do not depolarize in a material, so that the μSR time spectrum is independent of time, as shown in Fig. 1(a).

(9) In the case of a paramagnetic state where electron spins fluctuate fast, muons feel zero field on the time average of dipole fields due to electron spins. In this case, instead of the insensibility to electron dipole fields, muons feel nuclear dipole fields. Since nuclear spins fluctuate very slowly and the lives of muons are very short, muons feel small static fields due to nuclear spins, making Larmor precessions with low frequencies. Since the static fields that muons feel are at random, $A(t)$ decreases from unity slowly, showing a convex time-dependence, as shown in Fig. 1(b). This means that the depolarization of polarized μ^+ spins is slow. Note that $A(t)$ is expressed by the static Kubo–Toyabe function $G_z(\Delta, t)$,[2)]

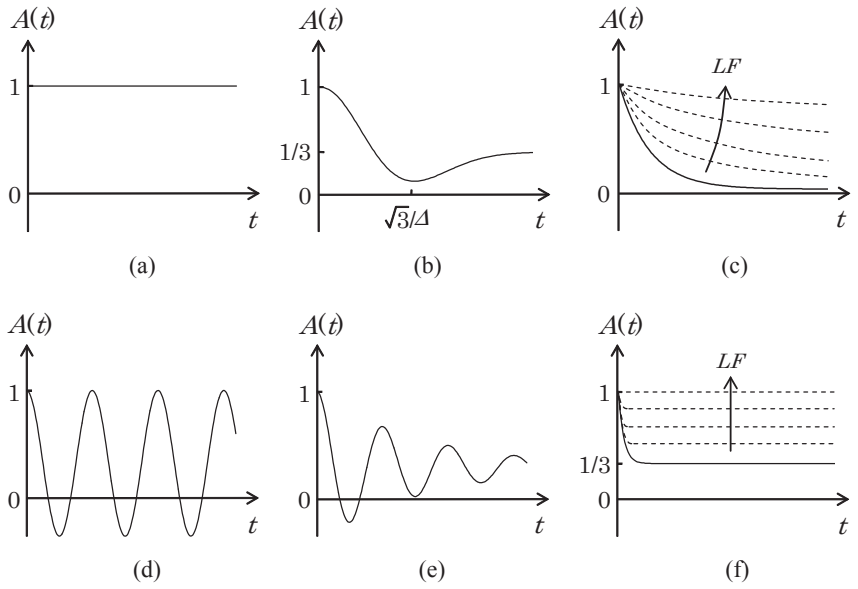

Fig. 1. Typical μSR time spectra. $A(t)$ is the asymmetry, namely, the polarization rate of μ^+ spins at time t. $A(0) = 1$. (a) In the case of no internal magnetic field. (b) In the case that the internal magnetic field is static and at random and that its distribution is Gaussian. This is the case when magnetic moments are comparatively dense in a material. $A(t)$ is expressed by the static Kubo–Toyabe function $G_z(\Delta, t)$,[2] where Δ is the full width at half maximum of the internal field distribution multiplied by γ_μ. (c) In the case that the internal magnetic field is dynamic, namely, dependent on time and space. Dashed lines indicate the recovery of the polarization rate of μ^+ spins with increasing longitudinal magnetic field LF. (d) In the case that the internal magnetic field is static and uniform. (e) In the case that the internal magnetic field is static and nonuniform. (f) In the case that the internal magnetic field is static and markedly at random and that its distribution is Lorentzian. This is the case when magnetic moments are comparatively dilute in a material. Dashed lines indicate the recovery of the polarization rate of μ^+ spins with increasing longitudinal magnetic field LF.

where Δ is the full width at half maximum of the internal field distribution multiplied by γ_μ.

(10) When the electron spin correlation is developed at low temperatures, electron spin fluctuations become slow, so that muons feel dipole fields due to electron spins, which are three orders of magnitude larger than nuclear dipole fields, making Larmor precessions with high frequencies. Since the fields that muons feel are at random and time-dependent, μ^+ spins depolarize rapidly, so that $A(t)$ shows a concave time dependence in a short-time region, as shown in Fig. 1(c). When a longitudinal magnetic field LF (parallel to the injection direction of muons) is applied, $A(t)$ recovers to unity, as shown by dashed lines in Fig. 1(c).

(11) When a long-range magnetic order is formed at much lower temperatures, muons feel large static fields, making Larmor precessions. In this case, when the stopping site of muons is single in the unit cell of a material, every muon feels the same internal field H, making a Larmor precession with the same period $t_{\rm osc} = 2\pi/\omega = 2\pi/(\gamma_\mu H)$. Accordingly, the μSR time spectrum shows an oscillation due to the muon-spin precession, as shown in Fig. 1(d). The internal field H can be estimated from $t_{\rm osc}$. This estimation is possible using a polycrystalline sample as well as a single-crystal sample of a material, because $t_{\rm osc}$ depends on not the direction of H but only the magnitude of H. When the magnitudes of H that muons feel are dispersive, the oscillation is damped as shown in Fig. 1(e). When the stopping site of muons is double in the unit cell of a material, the μSR time spectrum is composed of two kinds of oscillation with different $t_{\rm osc}$'s.

(12) When a short-range magnetic order such as a spin glass is formed at much lower temperatures, muons feel internal magnetic fields that are static but at random. Accordingly, the oscillation is damped fast, so that $A(t)$ decreases from unity to 1/3 rapidly, as shown in Fig. 1(f). The value of 1/3 is intuitively understood as follows. Since 1/3 of the static random fields are regarded as parallel to the injection direction of muons and 2/3 of those are regarded as perpendicular to it, 1/3 of muons make neither precession nor depolarization, while 2/3 of muons make precessions with various frequencies, leading to perfect depolarization. Accordingly, the average of the polarization rate of μ^+ spins becomes 1/3. When a longitudinal magnetic field is applied, $A(t)$ recovers to unity, as shown by dashed lines in Fig. 1(f).

3. μSR Studies on Magnetism in High-T_c Cuprates

3.1 Antiferromagnetic long-range ordered phase

At present, the highest superconducting transition temperature T_c among various kinds of cuprates is 134 K[3] (153 K under high pressure)[4] in $HgBa_2Ca_2Cu_3O_{8+\delta}$ of the so-called Hg1223 system. Every high-T_c cuprate includes two-dimensional CuO_2 planes in the crystal structure, which play a crucial role in the magnetism and superconductivity. It has been understood that the mother compounds of high-T_c cuprates, where Cu exists as Cu^{2+}, are Mott insulators owing to the strong electron correlation. Since Cu^{2+} has an electron spin (the spin quantum number $S = 1/2$) and the super-exchange interaction between Cu^{2+} spins via oxygen J is as large as 1500 K, mother compounds exhibit AF long-range order around room temperature. When mobile holes or electrons are doped into the CuO_2 plane, T_N decreases with increasing hole or electron concentration, the three-dimensional AF order disappears, and superconductivity appears, as shown in the phase diagram of Fig. 2. With heavy doping of holes or electrons, T_c decreases, followed by the appearance of a non-superconducting simple metallic state. Therefore, it is easily inferred that AF spin fluctuations may play an important role in the formation of Cooper pairs. Accordingly, it is significant to make a phase diagram such

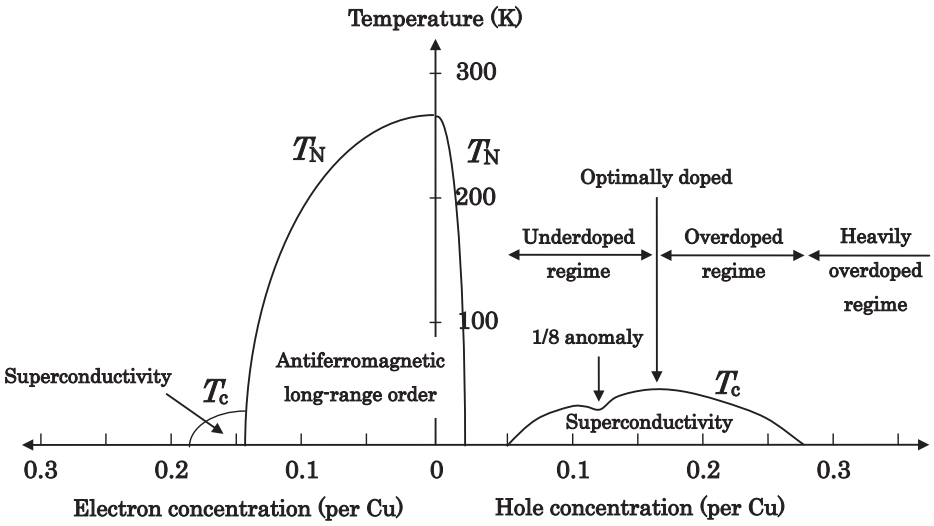

Fig. 2. Typical phase diagram of high-T_c cuprates. T_c and T_N are the superconducting transition temperature and Néel temperature, respectively. The 1/8 anomaly is marked in $La_{2-x}Ba_xCuO_4$, so that T_c decreases to zero at the hole concentration of 1/8 per Cu.

as Fig. 2, in order to investigate the mechanism of superconductivity.

μSR measurements have greatly contributed to the determination of the phase diagram, namely, the carrier concentration dependence of T_N in high-T_c cuprates,[5–15] because magnetic susceptibility measurements were useless. This is because the magnetic susceptibility exhibited little change at T_N owing to the development of two-dimensional AF correlation in the CuO_2 plane at high temperatures far above T_N except for the so-called La214 system. Figure 3 shows the μSR time spectra of $YBa_2Cu_3O_{6.2}$, which is nearly a mother compound of $YBa_2Cu_3O_{7-\delta}$ (YBCO) of the so-called Y123 system, in zero field by Nishida et al.[5] At 250 K, it is found that the depolarization of polarized μ^+ spins becomes fast and that an oscillation appears. The oscillation becomes clear at a low temperature of 15 K. As described at (11) in Sect. 2, the oscillation indicates the formation of a long-range magnetic order. Therefore, T_N is determined to be ~250 K in $YBa_2Cu_3O_{6.2}$. Similarly, phase diagrams of $Bi_2Sr_2Ca_{1-x}Y_xCu_2O_{8+\delta}$ of the so-called Bi2212 system[7,8] and $La_{2-x}Sr_xCuO_4$ (LSCO) of the La214 system[9,10] have been made by μSR measurements. As for electron-doped high-T_c cuprates, Luke et al.[11] and Fujita et al.[12] have made phase diagrams of $Nd_{2-x}Ce_xCuO_4$ (NCCO) and $Pr_{1-x}LaCe_x$-CuO_4 with the Nd_2CuO_4-type structure (so-called T′-type structure), respectively. In the so-called infinite-layer system, although no detailed phase diagram has been made, the magnetic transition temperature has been investigated in $Ca_{0.86}Sr_{0.14}CuO_2$[13] and $Sr_{0.9}La_{0.1}CuO_2$.[14,15] These studies are attributable to the merit of μSR measurements, that is, polycrystalline samples, which are prepared more easily than single crystals, are available for the measurements.

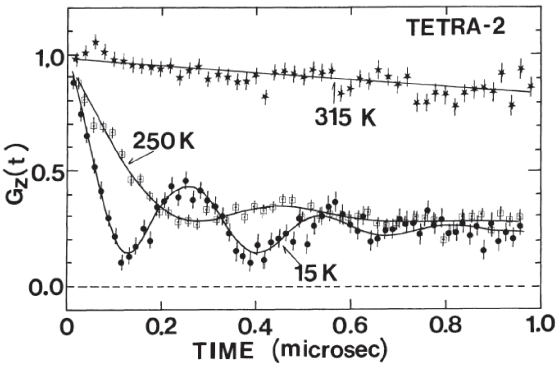

Fig. 3. μSR time spectra at 315, 250, and 15 K for $YBa_2Cu_3O_{6.2}$.[5]

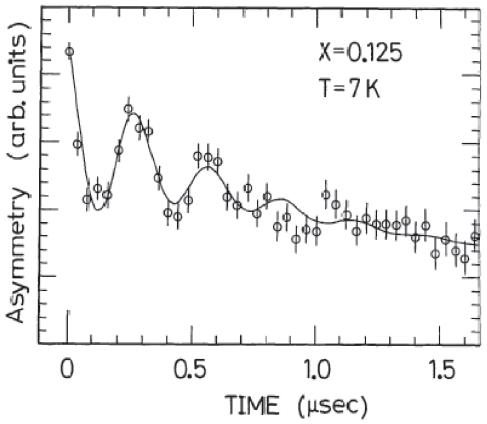

Fig. 4. μSR time spectrum at 7 K for $La_{2-x}Ba_xCuO_4$ ($x = 1/8$).[19]

3.2 1/8 anomaly and stripes

Just after the discovery of high-T_c superconductivity, the so-called 1/8 anomaly, namely, the anomalous suppression of superconductivity at the hole concentration per Cu, p, = 1/8 was found in $La_{2-x}Ba_xCuO_4$ (LBCO) of the La214 system, as shown in Fig. 2.[16–18] The origin of the 1/8 anomaly attracted great interest in relation to the origin of the high-T_c superconductivity, but it was not elucidated for a while. Thereat, μSR measurements by Watanabe et al.[19] have succeeded in observing a clear muon-spin precession in LBCO with $x = 1/8$, as shown in Fig. 4, using polycrystalline samples and revealed that the 1/8 anomaly is due to the formation of a long-range magnetic order. This is a distinguished result of μSR measurements. What was lucky is that polycrystalline samples were used for the μSR

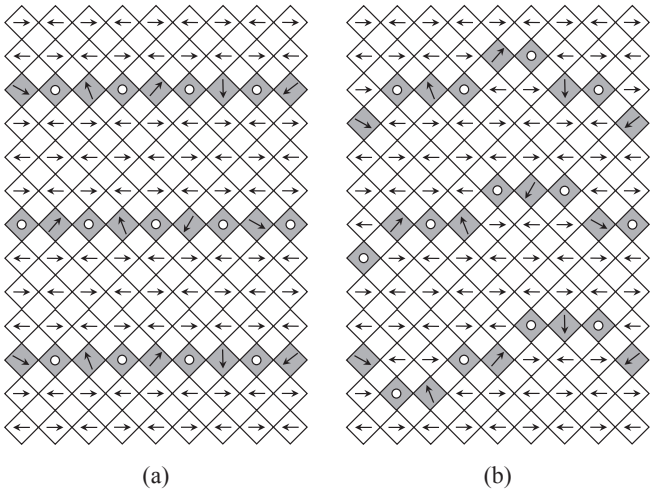

Fig. 5. (a) Static stripe order and (b) dynamically fluctuating stripes of Cu spins (↑) and holes (○) in the CuO_2 plane.

measurements, because no single crystal of LBCO with $x = 1/8$ was obtained in those days. Later, the long-range order was clarified to be a stripe order of Cu spins and holes, namely, a kind of SDW and CDW, as shown in Fig. 5(a), from the neutron scattering experiment using single crystals.[20] Here, note that, as a matter of fact, such a muon-spin precession as observed in LBCO with $x = 1/8$ had been observed in superconducting LSCO with $x = 0.11$ of the La214 system in μSR measurements by Torikai et al.[21] However, the result was not accepted so much at that time, because it was considered unusual that electrons in the CuO_2 plane contributed to both superconductivity and magnetic order. Later, the coexistence of superconductivity and magnetic order has been found in the underdoped regime of both LSCO and YBCO.[10,22,23] Even at present, this is a controversial issue.

The stripe order of Cu spins and holes is understood to be a well self-organized one so as to reduce the loss of both the magnetic energy between Cu spins and the kinetic energy of holes. It is true that the static stripe order suppresses the superconductivity, but it may be possible that dynamically fluctuating stripes of Cu spins and holes, as shown in Fig. 5(b), play an important role in the appearance of the high-T_c superconductivity as theoretically suggested by Kivelson et al.[24] If this is the case, the 1/8 anomaly should appear not only in LBCO and LSCO but also in the other high-T_c cuprates when adequate pinning centers to statically stabilize the dynamic stripes are introduced into a sample. In fact, by using Zn as pinning centers, the 1/8 anomaly has been found in partially Zn-substituted $Bi_2Sr_2Ca_{1-x}Y_x(Cu_{1-y}Zn_y)_2O_{8+\delta}$ of the Bi2212 system, as shown in Fig. 6.[25] Moreover, a fast depolarization of muon spins has been observed at low temperatures singularly at $p = 1/8$ per Cu in partially Zn-substituted $Bi_2Sr_2Ca_{1-x}Y_x(Cu_{1-y}Zn_y)_2O_{8+\delta}$, as shown in Figs. 6 and 7, although no muon-spin precession has been observed.[26,27] The fast depolarization is interpreted as being due to the slowing down of Cu-spin fluctuations toward the stabilization of a static stripe order, as described at (10) in Sect. 2. A similar 1/8 anomaly has been observed in μSR measurements of partially Zn-substituted $YBa_2Cu_{3-2y}Zn_{2y}O_{7-\delta}$ of the Y123 system, as shown in Fig. 8.[28] Recently, this μSR result has been reconfirmed, using

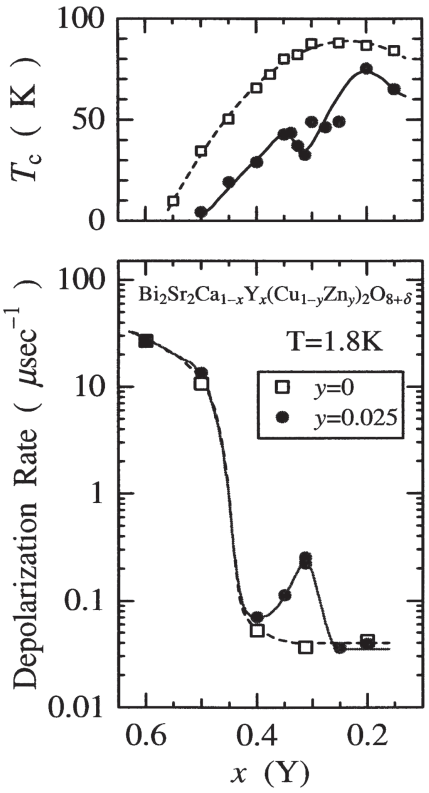

Fig. 6. x dependences of T_c and the depolarization rate of muon spins at 1.8 K for $Bi_2Sr_2Ca_{1-x}Y_x(Cu_{1-y}Zn_y)_2O_{8+\delta}$ ($y = 0, 0.025$).[25,27] At $x \sim 0.31$, the hole concentration is 1/8 per Cu.

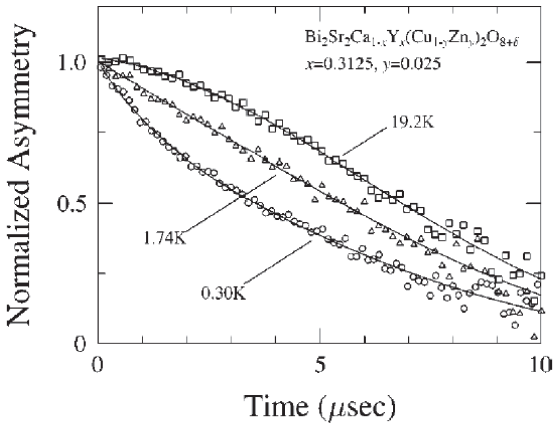

Fig. 7. μSR time spectra at various temperatures for $Bi_2Sr_2Ca_{1-x}Y_x(Cu_{1-y}Zn_y)_2O_{8+\delta}$ ($x = 0.3125$, $y = 0.025$) with the hole concentration of ~1/8 per Cu.[26]

detwinned single crystals of Zn-substituted $YBa_2(Cu_{0.98}Zn_{0.02})_3O_{6.6}$.[29] The Zn-induced magnetism at $p \sim 1/8$ in $YBa_2Cu_{3-2y}Zn_{2y}O_{7-\delta}$ has been found from NMR measurements also.[30,31] Accordingly, it is likely that the well-known 60 K plateau in the T_c vs $7 - \delta$ plot in YBCO is due to the 1/8 anomaly.[32–34] As for μSR studies on the 1/8 anomaly in the other hole-doped cuprates, the 1/8 anomaly has been observed in $La_{1.8}Nd_{0.2}CuO_{4+\delta}$, 1% Zn-substituted $La_{1.8}Nd_{0.2}Cu_{0.99}Zn_{0.01}O_{4+\delta}$, $La_{1.8}Pr_{0.2}CuO_{4+\delta}$, $La_{1.9}Eu_{0.1}CuO_{4+\delta}$, of the excess-oxygen-doped La214 system,[35–37] and also in 0.5% Zn-substituted $Ca_{2-x}Na_xCu_{0.995}Zn_{0.005}O_2Cl_2$ of the apical-halogen 214 system.[38] These results strongly suggest that the 1/8 anomaly and the dynamically fluctuating stripes of Cu

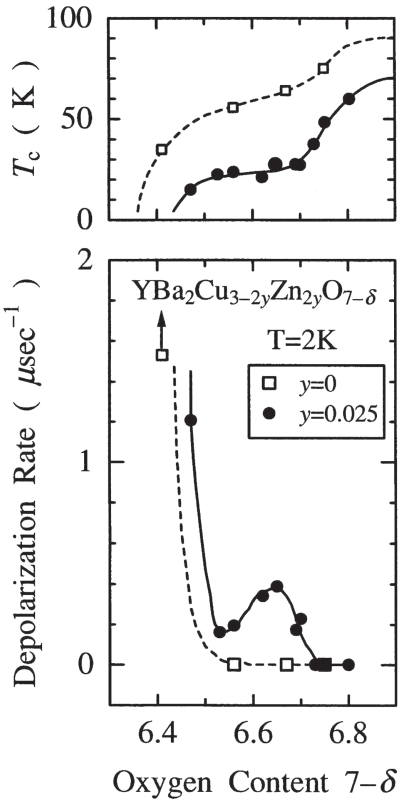

Fig. 8. Oxygen-content dependences of T_c and the depolarization rate of muon spins at 2 K for $YBa_2Cu_{3-2y}Zn_{2y}O_{7-\delta}$ ($y = 0, 0.025$).[28] At $7-\delta \sim 6.65$, the hole concentration is 1/8 per Cu.

spins and holes exist universally in hole-doped high-T_c cuprates.

As shown in Fig. 5(a), the stripe order of holes well matches with the crystal lattice at $p = 1/8$, so that the dynamically fluctuating stripes are inferred to be statically stabilized easily at $p = 1/8$. If the dynamic stripes play an important role in the appearance of high-T_c superconductivity, they should exist in a wide hole concentration range where the superconductivity emerges, and the pinning of the dynamic stripes, namely, the slowing down of Cu-spin fluctuations by the partial substitution of Zn for Cu should be observed not only at $p = 1/8$ but also in the wide hole concentration range. Therefore, μSR measurements have been carried out in a wide hole concentration range of partially Zn-substituted $La_{2-x}Sr_xCu_{1-y}Zn_yO_4$ ($0.10 \le x = p \le 0.30$) polycrystals.[39–42] As shown in Fig. 9, it has turned out that a fast depolarization of muon spins occurs at low temperatures through only 2–3% Zn substitution at $x = p \le 0.27$. At $x = 0.115$ and 0.10, a fast depolarization is observed even without Zn substitution owing to the marked 1/8 anomaly,[21] and an oscillation due to the muon-spin precession is observed through the substitution of a small amount of Zn, although the damping is strong. Through the substitution of a large amount of Zn, namely, the 10% Zn substitution, on the other hand, no fast depolarization is observed. This is inferred to be due to the destruction of the Cu-spin correlation caused by the dilution of Cu spins by a large amount of nonmagnetic Zn. Here, note that there were reports insisting that no fast depolarization was observed in μSR measurements at $x \ge 0.19$ in 1, 2, and 5% Zn-substituted $La_{2-x}Sr_xCu_{1-y}Zn_yO_4$,[43,44] but probably the amount of Zn

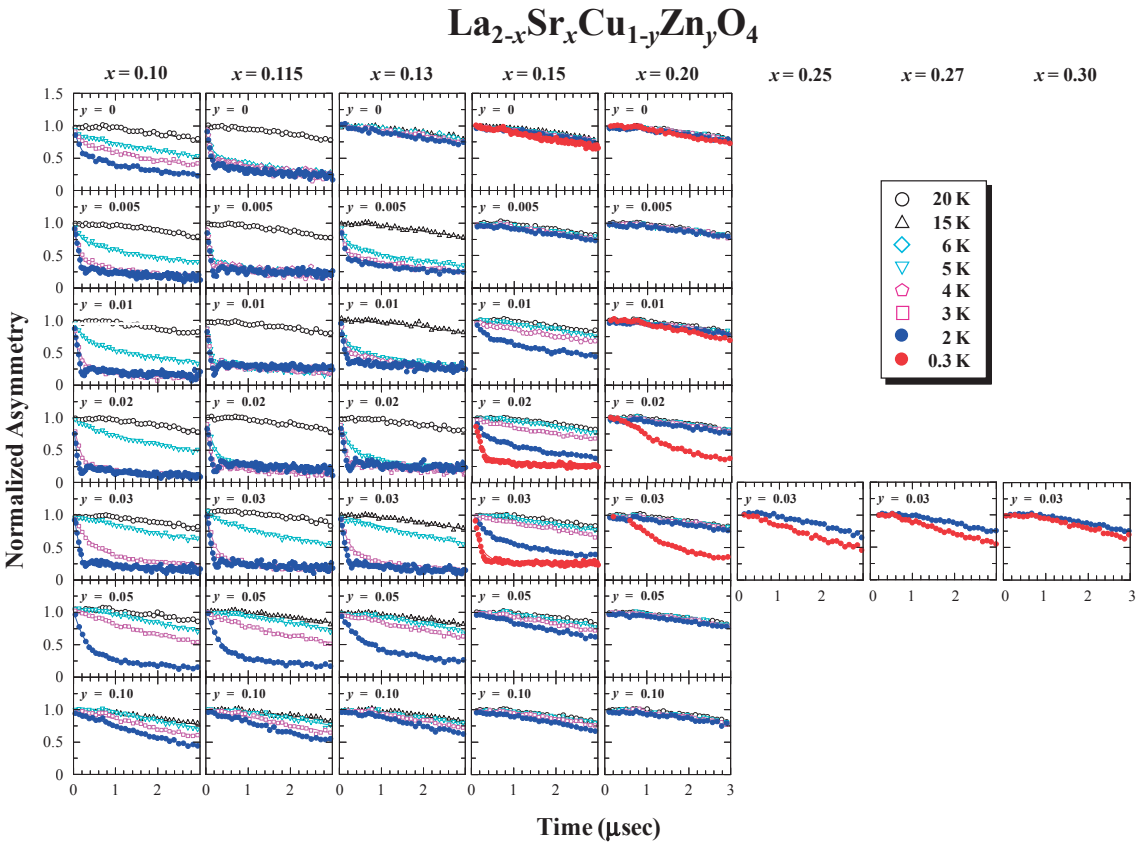

Fig. 9. (Color) μSR time spectra at various temperatures for $La_{2-x}Sr_xCu_{1-y}Zn_yO_4$ ($0.10 \le x \le 0.30$; $0 \le y \le 0.10$).[40–42]

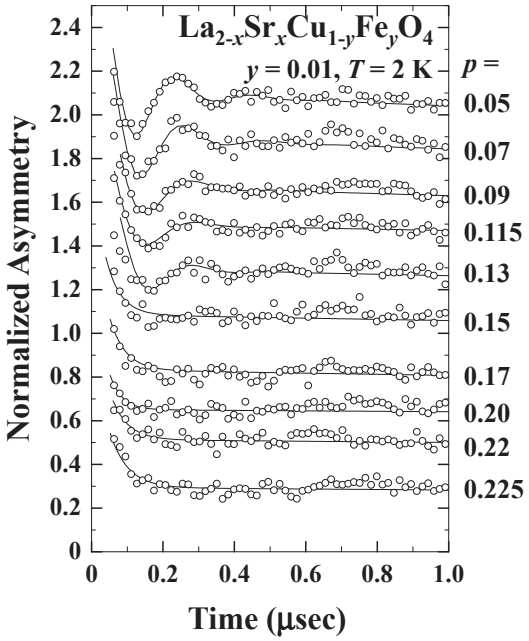

Fig. 10. μSR time spectra at 2 K for various hole concentrations per Cu, p, $= x - y$ in $La_{2-x}Sr_xCu_{1-y}Fe_yO_4$ ($y = 0.01$).[48] The spectra are shifted upward regularly 0.2 by 0.2 for clarity. The absence of data in a very short-time region below 0.05 μs is due to the use of a pulsed muon beam.

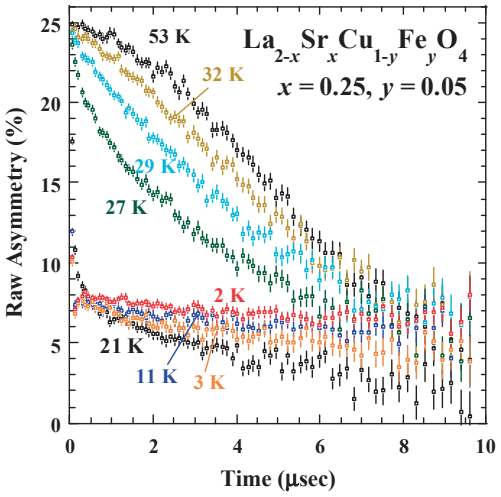

Fig. 11. (Color) μSR time spectra at various temperatures for $La_{2-x}Sr_xCu_{1-y}Fe_yO_4$ (the hole concentration per Cu, p, $= x - y = 0.20$; $y = 0.05$).[49]

was not suitable for the detection of the pinning of the dynamic stripes. In $Bi_{1.74}Pb_{0.38}Sr_{1.88}CuO_{6+\delta}$ of the so-called Bi2201 system also, a fast depolarization of muon spins has been observed at low temperatures through the 3% Zn substitution in a wide hole concentration range where the superconductivity emerges.[45] As expected, these results strongly suggest that a small amount of Zn operates to pin the dynamic stripes and that the dynamic stripes exist in the entire hole concentration range where the superconductivity emerges. Accordingly, it is possible that the dynamic stripes play an important role in the appearance of high-T_c superconductivity.

Later, it was clarified from the neutron scattering experiment by Fujita et al.[46] and the angle-resolved photoemission spectroscopy by He et al.[47] that the stripe order is stabilized at $p = 1/8$ in LSCO through the partial substitution of Fe for Cu more strongly than through the substitution of Zn and that an SDW state, which is different from the stripe-ordered state, is formed in the overdoped regime. Thereupon, μSR measurements have been performed in partially Fe-substituted $La_{2-x}Sr_xCu_{1-y}Fe_yO_4$ ($0.06 \le x \le 0.30$; $0 \le y \le 0.10$) polycrystals.[48,49] As shown in Fig. 10, it has turned out that a magnetic order occurs at low temperatures through only 1% Fe substitution in a wide range of x. What is characteristic is that an oscillation is observed in the underdoped regime of $p = x - y \lesssim 0.15$ ($p = x - y$, owing to +3 of the valence of Fe in the CuO_2 plane), while no oscillation is observed in the overdoped regime of $p \gtrsim 0.15$. The μSR time spectra in the underdoped and overdoped regimes are similar to those shown in Figs. 1(e) and 1(f), respectively. Moreover, it has been found that the magnetic transition temperature is not so dependent on the Fe content in the underdoped regime, while it increases with increasing Fe content in the overdoped regime. From these results, it has been concluded that magnetic Fe^{3+} with $S = 5/2$ pins the dynamic stripes more strongly than nonmagnetic Zn^{2+} in the underdoped regime, leading to the strong stabilization of the static stripe order. In the overdoped regime, on the other hand, it has been concluded that a spin-glass state of Fe^{3+} spins due to the RKKY interaction is formed. This means that the electronic state in the underdoped regime of hole-doped high-T_c cuprates is a strongly correlated one, while that in the overdoped regime is a weakly correlated Fermi-liquid one. The SDW state in the overdoped regime observed from the neutron scattering experiment[47] is attributable to the good nesting of the Fermi surface constructed by itinerant electrons and is not contradictory to the spin-glass state of Fe^{3+} spins. In fact, the spin-glass transition in the overdoped regime has been confirmed from the temperature dependence of the magnetic susceptibility in Fe-substituted $La_{2-x}Sr_xCu_{1-y}Fe_yO_4$ ($0.02 \le y \le 0.10$) with $p = 0.20$. Moreover, an unexpected transition has been found to occur at the temperature T_{g2}, which is lower than the spin-glass transition temperature T_{g1}. Thereupon, the μSR time spectra at various temperatures of 5% Fe-substituted $La_{2-x}Sr_xCu_{1-y}Fe_yO_4$ with $p = 0.20$ shown in Fig. 11 have been analyzed using the four-component function, $A(t) = A_0 e^{-\lambda_0 t} G_z(\Delta, t) + A_1 e^{-\lambda_1 t} + A_2 e^{-\lambda_2 t} \cos(\omega_2 t + \varphi_2) + A_3 e^{-\lambda_3 t} \cos(\omega_3 t + \varphi_3)$. Here, A_0, A_1, A_2, and A_3 are the initial asymmetries, and λ_0, λ_1, λ_2, and λ_3 are the depolarization rates of respective regions in a sample, and $G_z(\Delta, t)$ expresses the depolarization of μ^+ spins due to the nuclear dipole fields. As a result, it has been found that λ_0 shows two peaks at T_{g1} and T_{g2}, as shown in Fig. 12. That is, two kinds of magnetic transition have been found to occur from the magnetic susceptibility and μSR measurements. To study the origin of T_{g2}, the p dependence of T_{g2} has been investigated from the magnetic susceptibility measurements for 5% Fe-substituted $La_{2-x}Sr_xCu_{1-y}Fe_yO_4$. As a result, T_{g2} has been found to succeed to the magnetic transition in the underdoped regime, as shown in Fig. 13. Accordingly, it has been inferred that the high-temperature phase in the overdoped regime is a spin-glass one of Fe^{3+} spins mediated by itinerant electrons, while the low-temperature phase is a stripe-ordered one of Cu spins becoming more localized with decreasing temperature. In any case, the stripe-ordered phase of localized Cu spins is stabilized at low

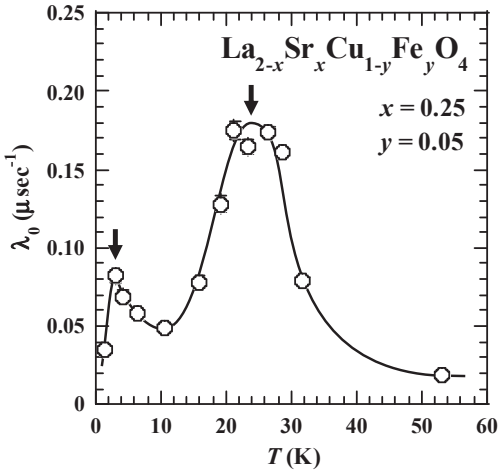

Fig. 12. Temperature dependence of the depolarization rate of the first term of the four-component function described in 3.2, λ_0, for $La_{2-x}Sr_xCu_{1-y}Fe_yO_4$ (the hole concentration per Cu, p, $= x - y = 0.20$; $y = 0.05$).[49] Arrows indicate magnetic transition temperatures.

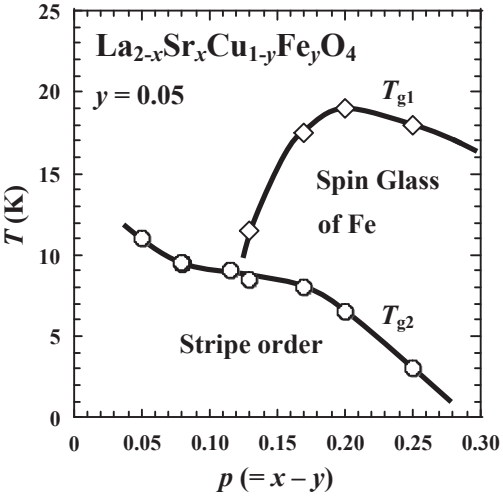

Fig. 13. Magnetic phase diagram of $La_{2-x}Sr_xCu_{1-y}Fe_yO_4$ ($y = 0.05$).[49] The hole concentration per Cu, p, $= x - y$.

temperatures through the partial substitution of Fe for Cu in the entire hole concentration range where the superconductivity emerges in LSCO. This strongly supports the above-described conclusion that the dynamic stripes exist in the entire hole concentration range where the superconductivity emerges and play an important role in the appearance of high-T_c superconductivity.

3.3 Impurity-induced magnetism

The study of the impurity effect on T_c is fundamental and important to elucidate the pairing mechanism of a superconductor. In fact, the impurity effect on T_c in hole-doped high-T_c cuprates is unconventional: nonmagnetic Zn decreases T_c more markedly than magnetic Ni.[50–52] Using μSR measurements, the reason has been investigated as follows. μSR measurements of Zn-substituted $La_{2-x}Sr_xCu_{1-y}Zn_yO_4$ and Ni-substituted $La_{2-x}Sr_xCu_{1-y}Ni_yO_4$ have revealed that the increase in the volume fraction of the magnetically ordered region through the Zn substitution is more marked than that through the Ni substitution, which has been in good correspondence to the decrease in the superconducting volume fraction estimated from the magnetic susceptibility measurements.[39–41,53–55] Therefore, it has been concluded that the superconductivity is destroyed like Swiss cheese around Zn and Ni, where dynamically fluctuating stripes of Cu spins and holes are pinned to be statically stabilized.[40,41,54,56] Moreover, it has been understood that nonmagnetic Zn^{2+} disturbs the Cu^{2+}-spin (with $S = 1/2$) state in the CuO_2 plane more strongly than magnetic Ni^{2+} (with $S = 1$), so that Zn^{2+} pins the dynamic stripes and destroys the superconductivity more markedly than Ni^{2+}. Thus, this scenario has succeeded in explaining the unconventional result of the impurity effect on T_c in hole-doped high-T_c cuprates.

As to the state of substituted Ni, later, it has been found that substituted Ni tends to trap a hole, forming a Zhang-Rice doublet state with the effective $S = 1/2$ similar to that of Cu^{2+} from neutron scattering,[57,58] magnetic susceptibility,[59] μSR,[60] x-ray absorption fine structure,[61] specific heat,[62,63] and a theoretical work using numerical exact diagonalization calculations.[64] This may be one reason why the effects of the Ni substitution are smaller than those of the Zn substitution. On the other hand, there is a report that the effects of the Zn and Ni substitutions on the superconductivity and magnetism are not very different from each other in the underdoped regime of LSCO, taking into account the hole trapping by Ni.[65]

μSR studies on the impurity-induced magnetism have greatly contributed to the investigation of the 1/8 anomaly and the impurity effect on T_c in hole-doped high-T_c cuprates, as described above. In electron-doped high-T_c cuprates, on the other hand, no impurity-induced magnetism has been observed.[66] The magnetic moments of constituent rare-earth ions in electron-doped high-T_c cuprates may obscure a possible change in Cu-spin fluctuations in the μSR measurements. Otherwise, dynamically fluctuating stripes of Cu spins and electrons may not exist in the CuO_2 plane, and the mechanism of the high-T_c superconductivity in electron-doped cuprates may be different from that in hole-doped cuprates.

3.4 Magnetic-field-induced magnetism

By μSR measurements in a transverse magnetic field *TF* (perpendicular to the injection direction of muons), magnetic-field-induced magnetism has been investigated in relation to the 1/8 anomaly and stripes in the La214 system. μSR measurements in *TF* up to 6 T parallel to the *c*-axis have revealed that field-induced quasi-static magnetism exists even at high temperatures above T_c (where superconducting fluctuations exist) and above the magnetic transition temperature, namely, the stripe-ordered temperature at $x = 0.12$ in LSCO, at $x = 1/8$ in LBCO and at $x = 0.15$ in Eu-substituted $La_{1.9-x}Eu_{0.1}Sr_xCuO_4$.[67] By taking into account the experimental results of neutron scattering,[68–73] x-ray scattering,[74] thermal conductivity,[75–77] and electrical resistivity,[78] it has been concluded that the field-induced magnetism is due to the stripe order of Cu spins and holes owing to the pinning of dynamically fluctuating stripes by vortex cores in the CuO_2 plane produced by the application of *TF* parallel to the *c*-axis. Moreover, it has been concluded that magnetic field effects on the stripes are small in samples where the stripes are well stabilized statically in zero field,

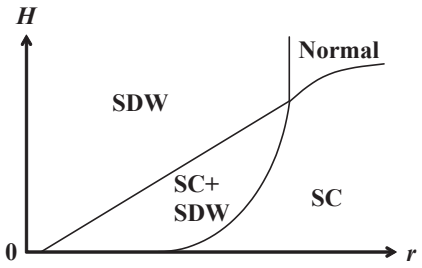

Fig. 14. Schematic phase diagram as functions of magnetic field and the parameter r, which is similar but not identical to the hole concentration, proposed by Demler et al.[81] SC denotes superconductivity.

such as LBCO with $x = 1/8$ and Nd-substituted $La_{1.6-x}Nd_{0.4}Sr_xCuO_4$ with $x = 0.15$, while the stripe order is developed by the application of a magnetic field parallel to the c-axis in samples where it is not well developed in zero field such as LSCO. This is plausible, because it is likely that vortex cores operate to induce spatial inhomogeneity in a superconductor to pin something, as well as impurities.

Apart from the 1/8 anomaly, μSR measurements have revealed that spin-glass-like magnetism is induced about vortex cores by the application of a magnetic field at $x = 0.145$ in LSCO, while no field-induced magnetism has been observed in overdoped LSCO with $x = 0.176$[79] nor with $x = 0.19$.[67] The spin-glass-like magnetism has been induced about vortex cores by the application of a magnetic field in underdoped YBCO with $7 - \delta = 6.50$ as well, but not in YBCO with $7 - \delta = 6.60$.[79] In optimally doped $Ca_{2-x}Na_xCuO_2Cl_2$ of the apical-halogen 214 system, field-induced magnetism has been observed even above T_c (where superconducting fluctuations exist) in the TF-μSR measurements.[80] On the other hand, no field-induced magnetism has been observed in optimally doped $(Bi,Pb)_2Sr_2CaCu_2O_8$ of the Bi2212 system nor 0.7% Zn-substituted $YBa_2(Cu_{0.993}Zn_{0.007})_3O_7$ in the TF-μSR measurements.[67] These results are understood fundamentally in terms of the phase diagram proposed by Demler et al.[81] as functions of magnetic field and the parameter r similar but not identical to the hole concentration, as shown in Fig. 14, based on the Ginzburg–Landau theory with competing AF and superconducting order parameters. That is, no observation of field-induced magnetism in the overdoped regime is regarded as being due to the location in the large-r region of Fig. 14. On the other hand, SDW in Fig. 14 is regarded as a part of the stripe order of Cu spins and holes, and there exist dynamically fluctuating stripes even in the overdoped regime as described in Sect. 3.2. Therefore, it is also possible to understand that these results are due to the pinning of the dynamically fluctuating stripes by vortex cores in the underdoped regime as well as impurities, leading to the development of the static stripe order, while the pinning of the stripes by vortex cores is insufficient to develop the static stripe order in the overdoped regime.

As for electron-doped cuprates, field-induced magnetism has been observed by Kadono et al.[82,83] in TF-μSR measurements of superconducting $Pr_{1-x}LaCe_xCuO_4$ with $x = 0.11$ and 0.15. The field-induced magnetism has been concluded to be AF order of induced small moments, which is not localized around vortices but uniform in the sample. This is in marked contrast to the field-induced magnetism in hole-doped cuprates, suggesting the difference in the electronic state between electron-doped and hole-doped cuprates. A similar field-induced magnetism has also been observed in TF-μSR measurements of superconducting $Pr_{2-x}Ce_xCuO_4$.[84]

3.5 *Pseudogap in hole-doped cuprates*

The so-called pseudogap behavior, namely, the decrease in the density of states at the Fermi level observed from NMR, photoemission spectroscopy, and so forth at high temperatures above T_c in the underdoped regime of hole-doped cuprates has attracted interest in relation to the origin of the high-T_c superconductivity. From the muon Knight shift in TF-μSR measurements, in fact, the opening of the pseudogap has been confirmed by Miyazaki et al.[85,86] at temperatures below ~250 K for underdoped $Bi_{1.76}Pb_{0.35}Sr_{1.89}CuO_{6+\delta}$ of the Bi2201 system.

There have been several candidates for the origin of the pseudogap such as incoherent preformed pairs, charge order, staggered flux phase, stripes, and so forth. Very precise μSR measurements in zero field at high temperatures in LSCO have revealed that the temperature T_μ, below which the Cu-spin fluctuations exhibit slowing down, is in good agreement with the temperature T_ρ, below which holes tend to be localized, estimated from the resistivity measurements.[87] These results are associated with the coupling of Cu spins and holes, namely, stripes of Cu spins and holes. Therefore, T_μ and T_ρ may be related to the formation of the stripe correlation or the slowing down of dynamically fluctuating stripes. Accordingly, it is possible that the stripes are related to the pseudogap. The details will be clarified by means of the other measurements in the future. In YBCO, μSR measurements in zero field have revealed that weak static magnetism occurs near the pseudogap transition temperature.[88] Besides, several μSR studies on the relation between the pseudogap and superconductivity or superconducting fluctuations have been reported.[89–91]

3.6 *Ferromagnetism in the heavily overdoped regime of hole-doped cuprates*

As to the non-superconducting heavily overdoped regime of hole-doped high-T_c cuprates as shown in Fig. 2, a theoretical study by Kopp et al.[92] has predicted the existence of a ferromagnetic order at low temperatures. This may be intuitively understood as being due to the increase in the density of states at the Fermi level toward the van Hove singularity with increasing hole concentration. If this is the case, the decrease in T_c in the overdoped regime of hole-doped cuprates can be interpreted as being due to ferromagnetic fluctuations. To detect the possible ferromagnetic order, Sonier et al.[93] have carried out μSR measurements using non-superconducting heavily overdoped LSCO single crystals with $x = 0.33$ and observed an enhancement of the depolarization rate of muon spins at very low temperatures below 0.9 K. Considering also the experimental results of the electrical resistivity and magnetic susceptibility, they have supported the theoretical prediction of the occurrence of weak localized ferromagnetism in the heavily overdoped regime. A similar enhancement of the depolarization rate of muon spins has also been observed at very low temperatures below 2 K in non-superconducting heavily overdoped $Bi_{1.74}Pb_{0.38}Sr_{1.88}CuO_{6+\delta}$ of the Bi2201 system.[45]

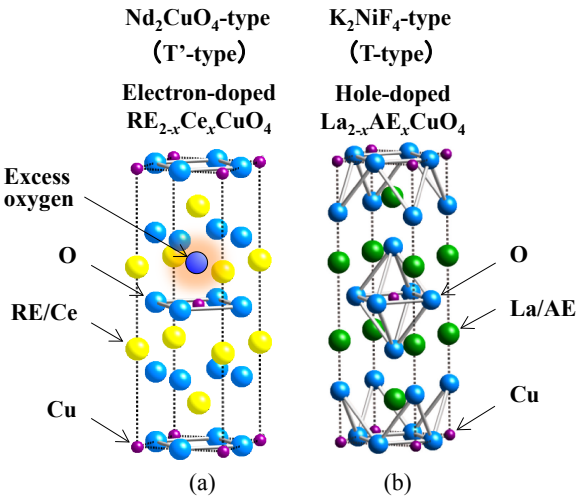

Fig. 15. (Color online) (a) Crystal structure of electron-doped high-T_c cuprates $RE_{2-x}Ce_xCuO_4$ (RE: rare-earth elements) with the Nd_2CuO_4-type (T′-type) structure. A small amount of excess oxygen occupies the apical site. (b) Crystal structure of hole-doped high-T_c cuprates $La_{2-x}AE_xCuO_4$ (AE: alkali earth metals) with the K_2NiF_4-type (T-type) structure.

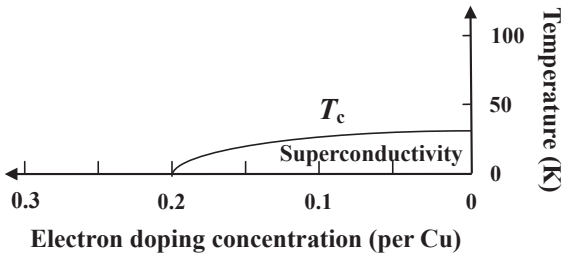

Fig. 16. Genuine phase diagram of electron-doped high-T_c cuprates. T_c is the superconducting transition temperature.

Of interest is that the enhancement of the depolarization is suppressed through the 3% Zn substitution, which is opposite to the Zn-substitution effect in the superconducting range of hole concentration in $Bi_{1.74}Pb_{0.38}Sr_{1.88}CuO_{6+\delta}$, as described in Sect. 3.2. In non-superconducting heavily overdoped $Bi_{1.74}Pb_{0.38}Sr_{1.88}CuO_{6+\delta}$, moreover, it has been found that both the electrical resistivity and magnetization exhibit behaviors characteristic of ferromagnetic fluctuations.[94] Accordingly, the existence of a ferromagnetic order at very low temperatures in the heavily overdoped regime of hole-doped cuprates seems true.

3.7 Undoped superconductivity in T′-type cuprates

In the electron-doped high-T_c cuprates $RE_{2-x}Ce_xCuO_4$ (RE: rare-earth elements) with the T′-type structure as shown in Fig. 15(a), it is well-known that the elimination of excess oxygen included at the apical site during the sample preparation is indispensable to the appearance of superconductivity. Recently, it has been found that AF long-range order disappears and superconductivity emerges even at $x = 0$, namely, without electron doping by means of the substitution of Ce for RE, in the case that the excess oxygen is adequately eliminated. This so-called undoped superconductivity in T′-type cuprates has been discovered by Naito's group using film samples, and the phase diagram of NCCO has been modified as shown in Fig. 16, which is quite different from that shown in Fig. 2.[95,96] The undoped superconductivity in T′-type cuprates has also been confirmed using bulk polycrystalline samples of $La_{2-x}Sm_xCuO_4$[97] and $La_{1.8}Eu_{0.2}CuO_4$ (LECO).[98] As for single-crystal samples, the undoped superconductivity has not yet been realized owing to the difficulty in eliminating excess oxygen without the decomposition of the crystal. However, superconducting single crystals of $Pr_{1.3-x}La_{0.7}Ce_xCuO_4$ (PLCCO) with $x = 0.10$ have been obtained by the so-called protect annealing method.[99]

At present, whether the origin of the undoped superconductivity in T′-type cuprates is the same as that in hole-doped curates attracts great interest. Thereupon, μSR measurements have been carried out using undoped LECO polycrystals and PLCCO single crystals with $x = 0.10$, to clarify whether the electronic state of T′-type cuprates is a strongly correlated one.[100] The μSR time spectra are shown in Fig. 17. For as-grown non-superconducting samples with excess oxygen, it is found that an oscillation is observed at low temperatures, as shown in Figs. 17(a) and 17(d), indicating the formation of AF long-range order. For the reduced superconducting sample of undoped LECO, on the other hand, the polarization rate of muon spins rapidly decreases from unity to $\sim 1/3$ and is flat in the long-time region at low temperatures, as shown in Fig. 17(b), although no oscillation is observed. By the application of *LF*, the flat spectrum in the long-time region recovers in parallel toward unity, as shown in Fig. 17(c). These μSR time spectra are similar to those shown in Fig. 1(f). Therefore, it has been found that short-range magnetic order is developed at low temperatures and coexists with the superconductivity. The development of the Cu-spin correlation has been observed by Kojima et al.[101] in undoped thin films of $La_{1.9}Y_{0.1}CuO_4$ also using slow muon beams. As for the reduced superconducting sample of PLCCO with $x = 0.10$, it has been found that the depolarization is slow at high temperatures, but it becomes fast with decreasing temperature and is of the exponential type at the lowest temperature of 3 K, as shown in Fig. 17(e). Looking into the spectra in the long-time region in detail shows that the asymmetry at 3 K is larger than that at 50 K. This indicates the existence of magnetically ordered regions in the sample at 3 K. Since no oscillation is observed at 3 K, no AF long-range order is formed in the sample. As shown in Fig. 17(f), μSR time spectra in *LF* are mixed ones of those shown in Figs. 1(c) and 1(f). Accordingly, it has been concluded that both short-range magnetically ordered regions and regions where Cu spins slowly fluctuate coexist in the sample.

μSR time spectra shown in Figs. 17(b) and 17(e) have been analyzed using the three-component function, $A(t) = A_0 e^{-\lambda_0 t} G_z(\Delta, t) + A_1 e^{-\lambda_1 t} + A_2 e^{-\lambda_2 t} \cos(\omega t + \varphi)$, and the two-component function, $A(t) = (A_0 e^{-\lambda_0 t} + A_1 e^{-\lambda_1 t}) \times \exp(-\sigma^2 t^2/2)$, respectively. Here, $\exp(-\sigma^2 t^2/2)$ expresses the depolarization of μ^+ spins due to the nuclear dipole fields as well as $G_z(\Delta, t)$. From the A_0, A_1, and A_2 values obtained by the analysis and the superconducting volume fraction estimated from the magnetic susceptibility and specific heat measurements, it has turned out that superconducting regions are overlapped with short-range magnetically ordered regions in the reduced superconducting samples of undoped LECO and PLCCO with $x = 0.10$.

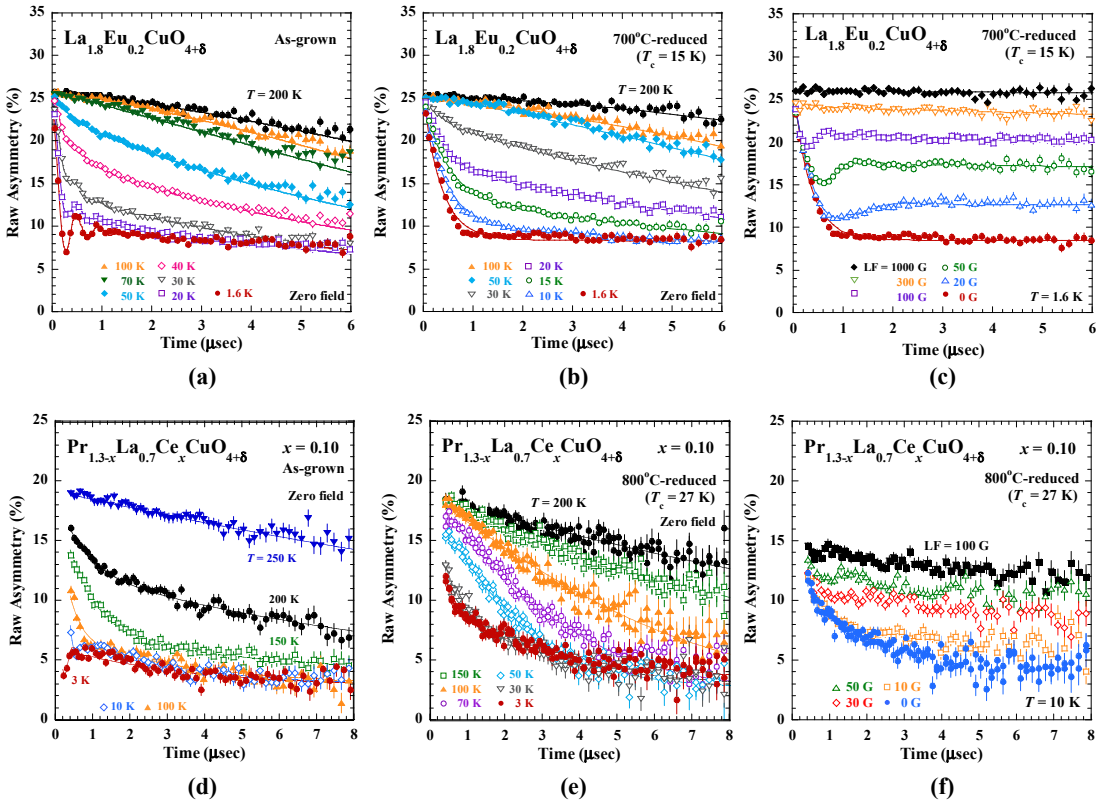

Fig. 17. (Color online) μSR time spectra at various temperatures for (a) as-grown $La_{1.8}Eu_{0.2}CuO_4$ (LECO), (b) reduced superconducting LECO, (c) reduced superconducting LECO in longitudinal magnetic field *LF*, (d) as-grown $Pr_{1.3-x}La_{0.7}Ce_xCuO_4$ (PLCCO) with $x = 0.10$, (e) reduced superconducting PLCCO with $x = 0.10$, and (f) reduced superconducting PLCCO with $x = 0.10$ in *LF*.[100] The absence of data in a very short-time region in (d)–(f) is due to the use of a pulsed muon beam.

These μSR results have suggested that the short-range magnetic order in the reduced superconducting samples is due to a tiny amount of excess oxygen, indicating that the electronic state of T′-type cuprates is a strongly correlated one. Therefore, it has been concluded that AF spin fluctuations may play an important role in the formation of Cooper pairs in the undoped superconductivity of T′-type cuprates as well as in the superconductivity of hole-doped curates.

Finally, note that the undoped superconductivity is understood as follows.[99] As described in Sect. 3.1, the electronic state of the mother compound of hole-doped high-T_c cuprates with the K_2NiF_4-type structure (the so-called T-type structure) shown in Fig. 15(b) is a Mott insulator based on the electronic structure with a charge-transfer gap between the upper Hubbard band (UHB) of Cu $3d_{x^2-y^2}$ and the O 2p band, as shown in Fig. 18(b). In the mother compound of electron-doped high-T_c cuprates with the T′-type structure shown in Fig. 15(a), on the other hand, the charge-transfer gap is closed as shown in Fig. 18(a) owing to the decrease in the energy of Cu $3d_{x^2-y^2}$. This is because Cu is surrounded by only four O^{2-} ions in the T′-type structure, while Cu is surrounded by six O^{2-} ions in the T-type structure. Accordingly, there exist both electrons of UHB of Cu $3d_{x^2-y^2}$ and holes of the O 2p band even in the mother compound with the T′-type structure, leading to metallic behavior and superconductivity.[99,102] As for the AF long-range order and short-range magnetic order in the as-grown samples, it has been inferred that they are stabilized due to the localization of holes and electrons caused by excess apical oxygen.

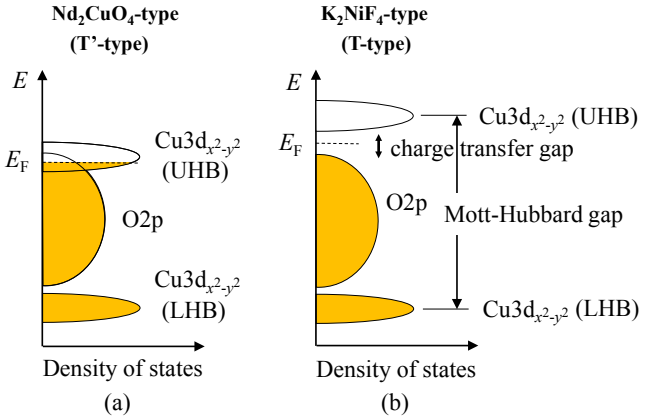

Fig. 18. (Color online) Electronic band structures of mother compounds of (a) electron-doped high-T_c cuprates with the Nd_2CuO_4-type (T′-type) structure and (b) hole-doped high-T_c cuprates with the K_2NiF_4-type (T-type) structure.

4. Conclusions

μSR studies on the magnetism in high-T_c cuprates have been reviewed. In particular, our studies on the 1/8 anomaly, stripes, and undoped superconductivity have been described in detail. In any case, μSR measurements have made great contributions to the understanding of the magnetism in high-T_c cuprates so far and even at present, making the most of the merit that polycrystalline samples are usable. Many foresighted results have been obtained from μSR measurements, followed by detailed studies by means of other experimental

techniques such as neutron scattering. Neutron scattering experiments require large-sized single crystals. NMR is not always usable on account of the difficulty of the signal detection. Therefore, it is considered that μSR measurements are very useful for detecting a possible magnetic anomaly or for investigating the spin state just after the discovery of a new material. The merit of μSR measurements, that is, polycrystalline samples are usable, makes it also easy to perform detailed studies by finely changing the concentration of components of a material, as carried out in partially Zn-substituted $La_{2-x}Sr_xCu_{1-y}Zn_yO_4$, as shown in Fig. 9. Moreover, μSR time spectra are easily obtained and interpreted on the magnetic state even by a μSR beginner as described in Sect. 2, if only polycrystalline samples were prepared. Accordingly, further use of μSR measurements is expected in material science.

*koike@teion.apph.tohoku.ac.jp

1) J. G. Bednorz and K. A. Müller, Z. Phys. B **64**, 189 (1986).
2) R. Kubo and T. Toyabe, in *Magnetic Resonance and Relaxation*, ed. R. Blinc (North-Holland, Amsterdam, 1967).
3) A. Schilling, M. Cantoni, J. D. Guo, and H. R. Ott, Nature **363**, 56 (1993).
4) N. Takeshita, A. Yamamoto, A. Iyo, and H. Eisaki, J. Phys. Soc. Jpn. **82**, 023711 (2013).
5) N. Nishida, H. Miyatake, D. Shimada, S. Okuma, M. Ishikawa, T. Takabatake, Y. Nakazawa, Y. Kuno, R. Keitel, J. H. Brewer, T. M. Riseman, D. Ll. Williams, Y. Watanabe, T. Yamazaki, K. Nishiyama, K. Nagamine, E. J. Ansaldo, and E. Torikai, Jpn. J. Appl. Phys. **26**, L1856 (1987).
6) N. Nishida, H. Miyatake, D. Shimada, S. Okuma, T. Yamazaki, Y. Watanabe, Y. Kuno, M. Ishikawa, T. Takabatake, K. Nagamine, K. Nishiyama, J. H. Brewer, and S. R. Kreitzmann, Physica C **153–155**, 761 (1988).
7) N. Nishida, H. Miyatake, S. Okuma, T. Tamegai, Y. Iye, R. Yoshizaki, K. Nishiyama, and K. Nagamine, Physica C **156**, 625 (1988).
8) N. Nishida, S. Okuma, H. Miyatake, T. Tamegai, Y. Iye, R. Yoshizaki, K. Nishiyama, K. Nagamine, R. Kadono, and J. H. Brewer, Physica C **168**, 23 (1990).
9) J. I. Budnick, B. Chamberland, D. P. Yang, Ch. Niedermayer, A. Golnik, E. Recknagel, M. Rossmanith, and A. Weidinger, Europhys. Lett. **5**, 651 (1988).
10) A. Weidinger, Ch. Niedermayer, A. Golnik, R. Simon, E. Recknagel, J. I. Budnick, B. Chamberland, and C. Baines, Phys. Rev. Lett. **62**, 102 (1989).
11) G. M. Luke, L. P. Le, B. J. Sternlieb, Y. J. Uemura, J. H. Brewer, R. Kadono, R. F. Kiefl, S. R. Kreitzman, T. M. Riseman, C. E. Stronach, M. R. Davis, S. Uchida, H. Takagi, Y. Tokura, H. Hidaka, T. Murakami, J. Gopalakrishnan, A. W. Sleight, M. A. Subramanian, E. A. Early, J. T. Markert, M. B. Maple, and C. L. Seaman, Phys. Rev. B **42**, 7981 (1990).
12) M. Fujita, T. Kubo, S. Kuroshima, T. Uefuji, K. Kawashima, K. Yamada, I. Watanabe, and K. Nagamine, Phys. Rev. B **67**, 014514 (2003).
13) A. Keren, L. P. Le, G. M. Luke, B. J. Sternlieb, W. D. Wu, and Y. J. Uemura, Phys. Rev. B **48**, 12926 (1993).
14) A. Shengelaya, R. Khasanov, D. G. Eshchenko, D. Di Castro, I. M. Savić, M. S. Park, K. H. Kim, S.-I. Lee, K. A. Müller, and H. Keller, Phys. Rev. Lett. **94**, 127001 (2005).
15) K. M. Kojima, K. Kawashima, M. Fujita, K. Yamada, M. Azuma, M. Takano, A. Koda, K. Ohishi, W. Higemoto, R. Kadono, and Y. J. Uemura, Physica B **374–375**, 207 (2006).
16) For a review, Y. Koike and T. Adachi, Physica C **481**, 115 (2012).
17) K. Kumagai, Y. Nakamura, I. Watanabe, Y. Nakamichi, and H. Nakajima, J. Magn. Magn. Mater. **76–77**, 601 (1988).
18) A. R. Moodenbaugh, Y. Xu, M. Suenaga, T. J. Folkerts, and R. N. Shelton, Phys. Rev. B **38**, 4596 (1988).
19) I. Watanabe, K. Kawano, K. Kumagai, K. Nishiyama, and K. Nagamine, J. Phys. Soc. Jpn. **61**, 3058 (1992).
20) J. M. Tranquada, B. J. Sternlieb, J. D. Axe, Y. Nakamura, and S. Uchida, Nature **375**, 561 (1995).
21) E. Torikai, I. Tanaka, H. Kojima, K. Kitazawa, and K. Nagamine, Hyperfine Interactions **63**, 271 (1991).
22) Ch. Niedermayer, C. Bernhard, T. Blasius, A. Golnik, A. Moodenbaugh, and J. I. Budnick, Phys. Rev. Lett. **80**, 3843 (1998).
23) S. Sanna, G. Allodi, G. Concas, A. D. Hillier, and R. De Renzi, Phys. Rev. Lett. **93**, 207001 (2004).
24) S. A. Kivelson, E. Fradkin, and V. J. Emery, Nature **393**, 550 (1998).
25) M. Akoshima, T. Noji, Y. Ono, and Y. Koike, Phys. Rev. B **57**, 7491 (1998).
26) I. Watanabe, M. Akoshima, Y. Koike, and K. Nagamine, Phys. Rev. B **60**, R9955 (1999).
27) I. Watanabe, M. Akoshima, Y. Koike, S. Ohira, and K. Nagamine, Phys. Rev. B **62**, 14524 (2000).
28) M. Akoshima, Y. Koike, I. Watanabe, and K. Nagamine, Phys. Rev. B **62**, 6761 (2000).
29) A. Suchaneck, V. Hinkov, D. Haug, L. Schulz, C. Bernhard, A. Ivanov, K. Hradil, C. T. Lin, P. Bourges, B. Keimer, and Y. Sidis, Phys. Rev. Lett. **105**, 037207 (2010).
30) A. V. Mahajan, H. Alloul, G. Collin, and J. F. Marucco, Phys. Rev. Lett. **72**, 3100 (1994).
31) M.-H. Julien, T. Fehér, M. Horvatić, C. Berthier, O. N. Bakharev, P. Ségransan, G. Collin, and J.-F. Marucco, Phys. Rev. Lett. **84**, 3422 (2000).
32) J. L. Tallon, G. V. M. Williams, N. E. Flower, and C. Bernhard, Physica C **282–287**, 236 (1997).
33) M. Akoshima and Y. Koike, J. Phys. Soc. Jpn. **67**, 3653 (1998).
34) R. Liang, D. A. Bonn, and W. N. Hardy, Phys. Rev. B **73**, 180505(R) (2006).
35) H. Mikuni, T. Adachi, S. Yairi, M. Kato, Y. Koike, I. Watanabe, and K. Nagamine, Phys. Rev. B **68**, 024524 (2003).
36) I. Watanabe, N. Oki, T. Adachi, H. Mikuni, Y. Koike, F. L. Pratt, and K. Nagamine, Phys. Rev. B **73**, 134506 (2006).
37) T. Adachi, Y. Koike, Risdiana, N. Oki, H. Mikuni, I. Watanabe, and F. L. Pratt, Physica C **460–462**, 1169 (2007).
38) K. H. Satoh, M. Hiraishi, M. Miyazaki, S. Takeshita, A. Koda, R. Kadono, I. Yamada, K. Oka, M. Azuma, Y. Shimakawa, and M. Takano, Physica B **404**, 713 (2009).
39) I. Watanabe, T. Adachi, K. Takahashi, S. Yairi, Y. Koike, and K. Nagamine, Phys. Rev. B **65**, 180516(R) (2002).
40) T. Adachi, S. Yairi, K. Takahashi, Y. Koike, I. Watanabe, and K. Nagamine, Phys. Rev. B **69**, 184507 (2004).
41) T. Adachi, N. Oki, Risdiana, S. Yairi, Y. Koike, and I. Watanabe, Phys. Rev. B **78**, 134515 (2008).
42) Risdiana, T. Adachi, N. Oki, S. Yairi, Y. Tanabe, K. Omori, Y. Koike, T. Suzuki, I. Watanabe, A. Koda, and W. Higemoto, Phys. Rev. B **77**, 054516 (2008).
43) C. Panagopoulos, J. L. Tallon, B. D. Rainford, T. Xiang, J. R. Cooper, and C. A. Scott, Phys. Rev. B **66**, 064501 (2002).
44) C. Panagopoulos, A. P. Petrovic, A. D. Hillier, J. L. Tallon, C. A. Scott, and B. D. Rainford, Phys. Rev. B **69**, 144510 (2004).
45) T. Adachi, Y. Tanabe, K. Suzuki, Y. Koike, T. Suzuki, T. Kawamata, and I. Watanabe, Phys. Rev. B **83**, 184522 (2011).
46) M. Fujita, M. Enoki, and K. Yamada, J. Phys. Chem. Solids **69**, 3167 (2008).
47) R.-H. He, M. Fujita, M. Enoki, M. Hashimoto, S. Iikubo, S.-K. Mo, H. Yao, T. Adachi, Y. Koike, Z. Hussain, Z.-X. Shen, and K. Yamada, Phys. Rev. Lett. **107**, 127002 (2011).
48) K. M. Suzuki, T. Adachi, Y. Tanabe, H. Sato, Y. Koike, Risdiana, Y. Ishii, T. Suzuki, and I. Watanabe, Phys. Rev. B **86**, 014522 (2012).
49) K. M. Suzuki, T. Adachi, H. Sato, I. Watanabe, and Y. Koike, arXiv:1503.04902.
50) G. Xiao, M. Z. Cieplak, J. Q. Xiao, and C. L. Chien, Phys. Rev. B **42**, 8752 (1990).
51) Y. Koike, N. Watanabe, T. Noji, and Y. Saito, Solid State Commun. **78**, 511 (1991).
52) Y. Koike, A. Kobayashi, T. Kawaguchi, M. Kato, T. Noji, Y. Ono, T. Hikita, and Y. Saito, Solid State Commun. **82**, 889 (1992).
53) I. Watanabe and K. Nagamine, Physica B **259–261**, 544 (1999).

54) T. Adachi, S. Yairi, Y. Koike, I. Watanabe, and K. Nagamine, Phys. Rev. B **70**, 060504(R) (2004).
55) Y. Koike, T. Adachi, N. Oki, Risdiana, M. Yamazaki, T. Kawamata, T. Noji, K. Kudo, N. Kobayashi, I. Watanabe, and K. Nagamine, Physica C **426–431**, 189 (2005).
56) B. Nachumi, A. Keren, K. Kojima, M. Larkin, G. M. Luke, J. Merrin, O. Tchernyshöv, Y. J. Uemura, N. Ichikawa, M. Goto, and S. Uchida, Phys. Rev. Lett. **77**, 5421 (1996).
57) M. Matsuda, M. Fujita, and K. Yamada, Phys. Rev. B **73**, 140503(R) (2006).
58) H. Hiraka, S. Ohta, S. Wakimoto, M. Matsuda, and K. Yamada, J. Phys. Soc. Jpn. **76**, 074703 (2007).
59) T. Machi, I. Kato, R. Hareyama, N. Watanabe, Y. Itoh, N. Koshizuka, S. Arai, and M. Murakami, Physica C **388–389**, 233 (2003).
60) Y. Tanabe, T. Adachi, Risdiana, T. Kawamata, T. Suzuki, I. Watanabe, and Y. Koike, Physica B **404**, 717 (2009).
61) H. Hiraka, D. Matsumura, Y. Nishihata, J. Mizuki, and K. Yamada, Phys. Rev. Lett. **102**, 037002 (2009).
62) Y. Tanabe, K. Suzuki, T. Adachi, Y. Koike, T. Kawamata, Risdiana, T. Suzuki, and I. Watanabe, J. Phys. Soc. Jpn. **79**, 023706 (2010).
63) K. Suzuki, T. Adachi, Y. Tanabe, Y. Koike, T. Kawamata, Risdiana, T. Suzuki, and I. Watanabe, Phys. Rev. B **82**, 054519 (2010).
64) K. Tsutsui, A. Toyama, T. Tohyama, and S. Maekawa, Phys. Rev. B **80**, 224519 (2009).
65) Y. Tanabe, T. Adachi, K. Suzuki, T. Kawamata, Risdiana, T. Suzuki, I. Watanabe, and Y. Koike, Phys. Rev. B **83**, 144521 (2011).
66) Risdiana, T. Adachi, N. Oki, Y. Koike, T. Suzuki, and I. Watanabe, Phys. Rev. B **82**, 014506 (2010).
67) A. T. Savici, A. Fukaya, I. M. Gat-Malureanu, T. Ito, P. L. Russo, Y. J. Uemura, C. R. Wiebe, P. P. Kyriakou, G. J. MacDougall, M. T. Rovers, G. M. Luke, K. M. Kojima, M. Goto, S. Uchida, R. Kadono, K. Yamada, S. Tajima, T. Masui, H. Eisaki, N. Kaneko, M. Greven, and G. D. Gu, Phys. Rev. Lett. **95**, 157001 (2005).
68) S. Katano, M. Sato, K. Yamada, T. Suzuki, and T. Fukase, Phys. Rev. B **62**, R14677 (2000).
69) B. Lake, H. M. Rønnow, N. B. Christensen, G. Aeppli, K. Lefmann, D. F. McMorrow, P. Vorderwisch, P. Smeibidl, N. Mangkorntong, T. Sasagawa, M. Nohara, H. Takagi, and T. E. Mason, Nature **415**, 299 (2002).
70) B. Lake, K. Lefmann, N. B. Christensen, G. Aeppli, D. F. McMorrow, H. M. Ronnow, P. Vorderwisch, P. Smeibidl, N. Mangkorntong, T. Sasagawa, M. Nohara, and H. Takagi, Nat. Mater. **4**, 658 (2005).
71) M. Fujita, M. Matsuda, H. Goka, T. Adachi, Y. Koike, and K. Yamada, J. Phys.: Conf. Ser. **51**, 510 (2006).
72) J. Wen, Z. Xu, G. Xu, J. M. Tranquada, and G. Gu, Phys. Rev. B **78**, 212506 (2008).
73) S. Wakimoto, R. J. Birgeneau, Y. Fujimaki, N. Ichikawa, T. Kasuga, Y. J. Kim, K. M. Kojima, S.-H. Lee, H. Niko, J. M. Tranquada, S. Uchida, and M. v. Zimmermann, Phys. Rev. B **67**, 184419 (2003).
74) J. Kim, A. Kagedan, G. D. Gu, C. S. Nelson, and Y.-J. Kim, Phys. Rev. B **77**, 180513(R) (2008).
75) K. Kudo, M. Yamazaki, T. Kawamata, T. Adachi, T. Noji, Y. Koike, T. Nishizaki, and N. Kobayashi, Phys. Rev. B **70**, 014503 (2004).
76) T. Kawamata, M. Yamazaki, N. Takahashi, T. Adachi, T. Noji, Y. Koike, K. Kudo, and N. Kobayashi, Physica C **426–431**, 469 (2005).
77) T. Kawamata, N. Takahashi, M. Yamazaki, T. Adachi, T. Manabe, T. Noji, Y. Koike, K. Kudo, and N. Kobayashi, AIP Conf. Proc. **850**, 431 (2006).
78) T. Adachi, N. Kitajima, T. Manabe, Y. Koike, K. Kudo, T. Sasaki, and N. Kobayashi, Phys. Rev. B **71**, 104516 (2005).
79) J. E. Sonier, F. D. Callaghan, Y. Ando, R. F. Kiefl, J. H. Brewer, C. V. Kaiser, V. Pacradouni, S. A. Sabok-Sayr, X. F. Sun, S. Komiya, W. N. Hardy, D. A. Bonn, and R. Liang, Phys. Rev. B **76**, 064522 (2007).
80) K. Ohishi, I. Yamada, A. Koda, S. R. Saha, R. Kadono, W. Higemoto, K. M. Kojima, M. Azuma, and M. Takano, arXiv:0910.5585.
81) E. Demler, S. Sachdev, and Y. Zhang, Phys. Rev. Lett. **87**, 067202 (2001).
82) R. Kadono, K. Ohishi, A. Koda, W. Higemoto, K. M. Kojima, M. Fujita, S. Kuroshima, and K. Yamada, J. Phys. Soc. Jpn. **73**, 2944 (2004).
83) R. Kadono, K. Ohishi, A. Koda, S. R. Saha, W. Higemoto, M. Fujita, and K. Yamada, J. Phys. Soc. Jpn. **74**, 2806 (2005).
84) J. E. Sonier, K. F. Poon, G. M. Luke, P. Kyriakou, R. I. Miller, R. Liang, C. R. Wiebe, P. Fournier, and R. L. Greene, Phys. Rev. Lett. **91**, 147002 (2003).
85) M. Miyazaki, R. Kadono, M. Hiraishi, K. H. Satoh, S. Takeshita, A. Koda, Y. Fukunaga, Y. Tanabe, T. Adachi, and Y. Koike, Physica C **470**, S55 (2010).
86) M. Miyazaki, R. Kadono, M. Hiraishi, A. Koda, K. M. Kojima, Y. Fukunaga, Y. Tanabe, T. Adachi, and Y. Koike, submitted.
87) I. Watanabe, T. Adachi, S. Yairi, Y. Koike, and K. Nagamine, J. Phys. Soc. Jpn. **77**, 124716 (2008) [Errata **78**, 028001 (2008)].
88) J. E. Sonier, J. H. Brewer, R. F. Kiefl, R. I. Miller, G. D. Morris, C. E. Stronach, J. S. Gardner, S. R. Dunsiger, D. A. Bonn, W. N. Hardy, R. Liang, and R. H. Heffner, Science **292**, 1692 (2001).
89) J. E. Sonier, M. Ilton, V. Pacradouni, C. V. Kaiser, S. A. Sabok-Sayr, Y. Ando, S. Komiya, W. N. Hardy, D. A. Bonn, R. Liang, and W. A. Atkinson, Phys. Rev. Lett. **101**, 117001 (2008).
90) Z. Lotfi Mahyari, A. Cannell, E. V. L. de Mello, M. Ishikado, H. Eisaki, R. Liang, D. A. Bonn, and J. E. Sonier, Phys. Rev. B **88**, 144504 (2013).
91) Y. Tanabe, T. Adachi, K. M. Suzuki, M. Akoshima, S. Heguri, T. Kawamata, Y. Ishii, T. Suzuki, I. Watanabe, and Y. Koike, J. Phys. Soc. Jpn. **83**, 074707 (2014).
92) A. Kopp, A. Ghosal, and S. Chakravarty, Proc. Natl. Acad. Sci. U.S.A. **104**, 6123 (2007).
93) J. E. Sonier, C. V. Kaiser, V. Pacradouni, S. A. Sabok-Sayr, C. Cochrane, D. E. MacLaughlin, S. Komiya, and N. E. Hussey, Proc. Natl. Acad. Sci. U.S.A. **107**, 17131 (2010).
94) K. Kurashima, T. Adachi, K. M. Suzuki, Y. Fukunaga, T. Kawamata, T. Noji, and Y. Koike, J. Phys.: Conf. Ser. **568**, 022003 (2014).
95) A. Tsukada, Y. Krockenberger, M. Noda, H. Yamamoto, D. Manske, L. Alff, and M. Naito, Solid State Commun. **133**, 427 (2005).
96) O. Matsumoto, A. Utsuki, A. Tsukada, H. Yamamoto, T. Manabe, and M. Naito, Physica C **469**, 924 (2009).
97) S. Asai, S. Ueda, and M. Naito, Physica C **471**, 682 (2011).
98) T. Takamatsu, M. Kato, T. Noji, and Y. Koike, Appl. Phys. Express **5**, 073101 (2012).
99) T. Adachi, Y. Mori, A. Takahashi, M. Kato, T. Nishizaki, T. Sasaki, N. Kobayashi, and Y. Koike, J. Phys. Soc. Jpn. **82**, 063713 (2013).
100) T. Adachi, A. Takahashi, K. M. Suzuki, M. A. Malik, T. Konno, T. Takamatsu, M. Kato, I. Watanabe, A. Koda, M. Miyazaki, R. Kadono, and Y. Koike, arXiv:1512.08095.
101) K. M. Kojima, Y. Krockenberger, I. Yamauchi, M. Miyazaki, M. Hiraishi, A. Koda, R. Kadono, R. Kumai, H. Yamamoto, A. Ikeda, and M. Naito, Phys. Rev. B **89**, 180508(R) (2014).
102) M. Naito, O. Matsumoto, A. Utsuki, A. Tsukada, H. Yamamoto, and T. Manabe, J. Phys.: Conf. Ser. **108**, 012037 (2008).

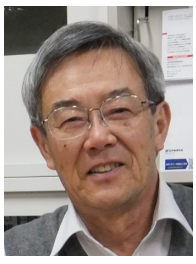

Yoji Koike was born in Ehime Prefecture, Japan in 1952. He obtained his B.Sc. (1975), M.Sc. (1977), and D.Sc. (1980) degrees from the University of Tokyo. He was a research associate at Institute for Materials Research, Tohoku University (1980–1989), and an associate professor (1989–1996), and a professor (1996–) at Department of Applied Physics, Tohoku University. During these periods, he was a visiting scientist at Technische Hochschule Darmstadt, Germany (1993). He has worked on experimental physics on superconductivity in intercalation compounds, high-T_c cuprates, iron-based superconductors, on Anderson localization, and on thermal conductivity in low-dimensional quantum spin systems.

Tadashi Adachi was born in Gunma Prefecture, Japan in 1973. He obtained his B.Eng. (1996), M.Eng. (1998), and D.Eng. (2001) degrees from the Tohoku University. He was a research associate and assistant professor at Department of Applied Physics, Tohoku University (2001–2013), and an associate professor (2013–) at Department of Engineering and Applied Sciences, Sophia University. During these periods, he was a visiting scientist at Simon Fraser University, Canada (2006–2007). He has worked on experimental physics on superconductivity in high-T_c cuprates and iron-chalcogenides.